

Finite element solution of mixed convection micropolar fluid flow between two vertical plates with varying temperature

L. KUMAR¹⁾, R. BHARGAVA¹⁾, P. BHARGAVA²⁾, H.S. TAKHAR³⁾

¹⁾*Department of Mathematics,
Indian Institute of Technology Roorkee, India*

²⁾*Department of Civil Engineering,
Indian Institute of Technology Roorkee, India*

³⁾*Department of Engineering,
Manchester Metropolitan University,
Manchester, M1 5 GD. U.K.
e-mail: H.S.Takhar@mmu.ac.uk*

THIS PAPER presents a finite element solution for the mixed convection micropolar fluid flow between two parallel plates with varying temperature. The governing differential equations are solved numerically using the finite element method. The effect of important parameters, namely pressure gradient, micropolar parameter and surface, condition parameter on velocity, microrotation as well as on temperature functions has been studied. It is noticed that the micropolar fluids act as a cooling agent as well as a drag reducing fluids.

Notations

| | |
|------------|--|
| f | dimensionless velocity function, |
| g | dimensionless microrotation, |
| T | temperature, |
| g_e | gravitational acceleration, |
| N | microrotation, |
| P | pressure, |
| ΔP | dimensionless pressure gradient, |
| Q | volumetric flow rate, |
| c | varying temperature factor, |
| x | streamwise coordinate, |
| y | normal coordinate, |
| u | velocity along the x -axis, |
| A | dimensionless microrotation parameter, |
| R | dimensionless micropolar parameter, |
| w_i | arbitrary test functions, |
| k_f | coefficient of thermal conductivity, |
| $2L$ | distance between the plates, |

- S dimensionless wall heat parameter,
 m wall heat ratio parameter; change in m produces unequal temperatures at the walls.

Greek letters

- η dimensionless coordinate perpendicular to the plates,
 μ dynamic viscosity,
 ρ density of the fluid,
 κ gyro-viscosity coefficient,
 γ micropolar parameter,
 θ dimensionless temperature,
 β volumetric coefficient of thermal expansion,
 ψ_i interpolation functions.

1. Introduction

ERINGEN [1] INTRODUCED THE CONCEPT of microfluids, which deals with a class of fluids, exhibiting certain microscopic effects arising from the local structure and micro-motions of the fluid elements. These fluids can support stress moments and body moments and are influenced by the spin inertia. Later ERINGEN [2] developed a subclass of these microfluids, called micropolar fluids, where the micro-rotational effects and micro-rotational inertia exist but they do not support stretch. They can support couple stresses and body couples only. Physically some polymeric fluids, fluids containing small amounts of polymeric additives, blood, paints, lubricating oils, liquid crystals, colloidal fluids and suspension fluid may be represented by the mathematical model, underlying micropolar fluids. An excellent review of micropolar fluids and their applications were provided by ARIMAN *et al.* [3].

HOYT and FABULA [4] have shown experimentally that the fluids containing minute polymeric additives indicate considerable reduction of the skin friction (about 25–30%); a concept, which is well explained by the theory of micropolar fluids. As an application, these fluids with microstructure are also capable of representing the body fluids.

The problems of micropolar fluid flow between two vertical plates (channel) are of great technical interest. A lot of attention has been given by many researchers. SASTRY and RAO [5] have studied the effect of suction in the laminar flow of a micropolar fluid in a channel, considering the Poiseuille flow at the entry of the channel. BHARGAVA and RANI [6] have examined the convective heat transfer in micropolar fluid flow between parallel plates. Its extension to free and forced convection is an interesting area of research including liquid crystals, dilute solutions of polymer fluids and many types of suspensions, since in many configurations in the technology and nature, one continually encounters masses of fluid rising freely in an extensive medium due to the buoyancy ef-

fects. AGARWAL and DHANAPAL [7] analyzed free convection micropolar fluid flow between two parallel porous vertical plates. The problem of fully developed free convection of a micropolar fluid in vertical channels has been discussed by CHAMKHA *et al.* [8]. SRINIVASACHARYA *et al.* [9] have investigated the problem of unsteady Stokes flow of micropolar fluid between two parallel porous plates. In a forced convection situation, natural convection effects are also present in the presence of gravitational body forces. The situation where both the natural and forced convection effects are of comparable order is called mixed or combined convection.

GORLA *et al.* [10] studied the fully developed laminar mixed convection flow of a micropolar fluid between two vertical parallel plates maintained at uniform but different temperatures. Excellent applications can be found in NIGAM *et al.* [11], where the authors discussed the problem of micropolar fluid film lubrication between two parallel plates with reference to human joints. One of the recent but excellent papers demonstrating the basic theories of micropolar fluids and its applications is that given by ŁUKASZEWICZ [12].

The purpose of the present paper is to analyze the mixed convection flow of a micropolar fluid between two vertical parallel plates with varying temperature. Such type of study may be applicable in nuclear reactors, heat exchangers and various electronic devices. Perhaps the most important question here is the effect of buoyancy on the forced convection transport rates. The buoyancy forces may aid or oppose the forced flow causing an increase or decrease in the heat transfer rates.

In this paper, the set of coupled nonlinear differential equations governing the flow, microrotation and temperature fields are solved by the finite element method and the results have been compared with those obtained by GORLA *et al.* [10]. A discussion is provided for the effect of the pressure gradient parameter, micropolar parameter and surface condition parameter on the flow, microrotation and temperature profiles. The influence of temperature on these functions, when it varies linearly along the x -axis, has been also discussed.

2. Mathematical analysis

Consider steady, laminar mixed convection flow of an incompressible micropolar fluid passing between two infinite vertical parallel plates. The plates are kept at a distance $2L$ apart, parallel to the direction of the gravitational body force. The x -axis extends along the plate and is located along the centerline of the channel, while the y -axis is normal to the plates. ' u ' is the velocity component along the x -axis, N – the component of microrotation and T – the temperature. Temperature is varying linearly along the x -axis with cx and $m cx$ being the temperatures of the left ($y = -L$) and the right-hand plate

($y = L$) respectively. Thus the governing equations of this type of flow can be written as:

Momentum:

$$(2.1) \quad (\mu + \kappa) \frac{d^2 u}{dy^2} + \kappa \frac{dN}{dy} - \frac{dP}{dx} + \rho g_e \beta T = 0.$$

Angular momentum:

$$(2.2) \quad \gamma \frac{d^2 N}{dy^2} - \kappa \frac{du}{dy} - 2\kappa N = 0.$$

Energy equation:

$$(2.3) \quad k_f \frac{d^2 T}{dy^2} + \left(\mu + \frac{\kappa}{2}\right) \left(\frac{du}{dy}\right)^2 + \frac{\kappa}{2} \left(\frac{du}{dy} + 2N\right)^2 + \gamma \left(\frac{dN}{dy}\right)^2 = 0.$$

The question of boundary conditions for structured fluids deserves some additional comments. Eringen suggested the no-spin boundary condition as being equivalent to a no-slip condition. This condition corresponds to strong concentration of microelements in the vicinity of the boundary. The physical interpretation is that there is a fluid-solid interface with strong interactions such that the microstructure does not rotate with respect to the surface.

The other boundary condition, suggested by AHMADI [13], corresponds to the condition that the antisymmetric part of the stress is zero on the surface, which requires that the particle spin should be equal to fluid vorticity at the boundary. In other words, in the neighborhood of a rigid boundary the effect of microstructure must be negligible since the suspended particles cannot get closer to the boundary than their radius. For example in the case of blood flow, it is observed that the red cells do not get very close to the boundary. Therefore, in the neighborhood of the boundary the only rotation is due to fluid shear and therefore, the gyration vector must be equal to the angular velocity. DAHLER and SCRIVEN [14] demonstrated that the general boundary conditions may have important applications.

KIRWAN [15] analysed a general linear relation between the microrotation rate and vorticity at the rigid boundaries given by:

$$N(x, 0) = -s \left(\frac{\partial u}{\partial y}\right)_{y=0},$$

where s is the surface condition parameter and it varies from 0 to 1.

Another important type of boundary condition explained by PEDDIESON [16] is the non-vanishing angular velocity at the boundary. Using this result,

GORLA [10] demonstrated that the micropolar fluid model is capable of predicting results, comparable to the characteristics found in turbulent flows. The boundary conditions similar to those used by GORLA [10], have been assumed here.

The appropriate physical boundary conditions are given by

$$(2.4) \quad \begin{aligned} y = -L : \quad u = 0, \quad N = N_o, \quad T = cx, \\ y = L : \quad u = 0, \quad N = N_o, \quad T = mcx, \end{aligned}$$

where m is the wall temperature ratio parameter and c is the varying temperature factor.

Introducing the dimensionless functions f , g and θ , defined by

$$(2.5) \quad \begin{aligned} \eta = \frac{y}{L}, \quad u = \frac{U_o}{S} f, \quad T = \frac{cL}{S} \theta, \\ N = \frac{U_o}{LS} g, \quad U_o = \frac{\rho g_e \beta L^3 c}{\mu}, \quad S = \frac{\mu U_o^2}{k_f c L}. \end{aligned}$$

The set of differential equations (2.1)–(2.3) can be written in the following form:

$$(2.6) \quad (1 + R) f'' + Rg' + \theta = \frac{\mu U_o^2}{k_f \rho g_e \beta (cL)^2} \frac{dP}{dx},$$

$$(2.7) \quad Ag'' - f' - 2g = 0,$$

$$(2.8) \quad \theta'' + \left(1 + \frac{R}{2}\right) f'^2 + \frac{R}{2} (f' + 2g)^2 + ARg'^2 = 0,$$

where $R = \kappa/\mu$ is the dimensionless micropolar parameter, $A = \gamma/\kappa L^2$ is the dimensionless microrotation parameter and $\Delta P = \frac{\mu U_o^2}{k_f \rho g_e \beta (cL)^2} \frac{dP}{dx}$ is the pressure gradient parameter.

Thus the condition: $\Delta P = 0 \Rightarrow \frac{dP}{dx} = 0$ corresponds to a free convection flow, while non-zero values of the pressure gradient correspond to a mixed convection flow.

The corresponding boundary conditions given in Eq. (2.10) reduce then to

$$(2.9) \quad \begin{aligned} \eta = -1; \quad f = 0, \quad g = \frac{LS}{U_o} N_o = g_o, \quad \theta = \frac{x}{L} S, \\ \eta = 1; \quad f = 0, \quad g = \frac{LS}{U_o} N_o = g_o, \quad \theta = m \frac{x}{L} S. \end{aligned}$$

The differential equations (2.14)–(3.5) with the boundary conditions as those given in (3.7) have been solved numerically using the finite element method for the different parameters, namely the pressure gradient parameter ΔP , micropolar parameter R , surface condition parameter g_o and variable x .

3. Method of solution

3.1. Finite element method

The set of differential equations given in Eqs. (2.14)–(3.5) are highly nonlinear therefore it cannot be solved analytically. Hence finite element method has been used in obtaining their solution. The steps involved in the finite-element analysis are as follows:

1. Division of the domain into linear elements, called the finite element mesh.
2. Generation of the element equations using variational formulations.
3. Assembly of the element equations as obtained in steps (2).
4. Introduction of the boundary conditions to the equations obtained in (3).
5. Solution of the assembled algebraic equations.

The assembled equations can be solved by any of the numerical technique viz. Gaussian elimination, LU Decomposition method etc. The details of the method used here can be studied in the paper given by REDDY [17].

3.2. Variational formulation:

The variational form associated with Eqs. (2.14) to (3.5) over a typical two-node linear element (η_e, η_{e+1}) is given by

$$(3.1) \quad \int_{\eta_e}^{\eta_{e+1}} w_1 \{ (1 + R) f'' + Rg' + \theta - \Delta P \} d\eta = 0,$$

$$(3.2) \quad \int_{\eta_e}^{\eta_{e+1}} w_2 \{ Ag'' - f' - 2g \} d\eta = 0,$$

$$(3.3) \quad \int_{\eta_e}^{\eta_{e+1}} w_3 \{ \theta'' + (1 + R) f'^2 + 2Rf'g + 2Rg^2 + ARg'^2 \} d\eta = 0,$$

where w_1 , w_2 and w_3 are the arbitrary test functions which may be viewed as the variations in the functions f , g and θ , respectively.

3.3. Finite element formulation

The finite element model may be obtained from (3.10)–(3.3) by substituting the finite element approximations of the form

$$(3.4) \quad f = \sum_{j=1}^2 f_j \psi_j, \quad g = \sum_{j=1}^2 g_j \psi_j, \quad \theta = \sum_{j=1}^2 \theta_j \psi_j$$

with

$$w_1 = w_2 = w_3 = \psi_i \quad (i = 1, 2,)$$

where ψ_i are the shape functions for a typical element (η_e, η_{e+1}) which are assumed in the form:

$$\psi_1^{(e)} = \frac{\eta_{e+1} - \eta}{\eta_{e+1} - \eta_e}, \quad \psi_2^{(e)} = \frac{\eta - \eta_e}{\eta_{e+1} - \eta_e}, \quad \eta_e \leq \eta \leq \eta_{e+1}.$$

The finite element model of the equations thus formed is the following:

$$(3.5) \quad \begin{bmatrix} [K^{11}] & [K^{12}] & [K^{13}] \\ [K^{21}] & [K^{22}] & [K^{23}] \\ [K^{31}] & [K^{32}] & [K^{33}] \end{bmatrix} \begin{bmatrix} \{f\} \\ \{g\} \\ \{\theta\} \end{bmatrix} = \begin{bmatrix} \{r^1\} \\ \{r^2\} \\ \{r^3\} \end{bmatrix}.$$

Here $[K^{mn}]$ and $[r^m]$ ($m, n = 1, 2, 3$) are the matrices of order 2×2 and 2×1 respectively, hence each matrix element is of the order 6×6 . The matrix $[K^{23}]$ is the null matrix, while the matrices $[K^{11}]$, $[K^{13}]$, $[K^{22}]$ and $[K^{33}]$ are symmetric matrices. All these matrices are defined as follows:

$$(3.6) \quad \begin{aligned} K_{ij}^{11} &= -(1+R) \int_{\eta_e}^{\eta_{e+1}} \frac{d\psi_i}{d\eta} \frac{d\psi_j}{d\eta} d\eta, & K_{ij}^{12} &= R \int_{\eta_e}^{\eta_{e+1}} \psi_i \frac{d\psi_j}{d\eta} d\eta, \\ K_{ij}^{13} &= \int_{\eta_e}^{\eta_{e+1}} \psi_i \psi_j d\eta & K_{ij}^{21} &= - \int_{\eta_e}^{\eta_{e+1}} \psi_i \frac{d\psi_j}{d\eta} d\eta, \\ K_{ij}^{22} &= -A \int_{\eta_e}^{\eta_{e+1}} \frac{d\psi_i}{d\eta} \frac{d\psi_j}{d\eta} d\eta - 2 \int_{\eta_e}^{\eta_{e+1}} \psi_i \psi_j d\eta, & K_{ij}^{23} &= 0, \\ K_{ij}^{31} &= (1+R) \int_{\eta_e}^{\eta_{e+1}} \psi_i \frac{d\bar{f}}{d\eta} \frac{d\psi_j}{d\eta} d\eta + 2R \int_{\eta_e}^{\eta_{e+1}} \psi_i \bar{g} \frac{d\psi_j}{d\eta} d\eta, \end{aligned}$$

$$\begin{aligned}
K_{ij}^{32} &= 2R \int_{\eta_e}^{\eta_{e+1}} \psi_i \bar{g} \psi_j d\eta + AR \int_{\eta_e}^{\eta_{e+1}} \psi_i \frac{d\bar{g}}{d\eta} \frac{d\psi_j}{d\eta} d\eta, \\
(3.6) \quad K_{ij}^{33} &= - \int_{\eta_e}^{\eta_{e+1}} \frac{d\psi_i}{d\eta} \frac{d\psi_j}{d\eta} d\eta, \quad r_i^1 = \int_{\eta_e}^{\eta_{e+1}} \Delta P \psi_i d\eta - (1+R) \left(\psi_i \frac{df}{d\eta} \right)_{\eta_e}^{n_{e+1}}, \\
r_i^2 &= -A \left(\psi_i \frac{dg}{d\eta} \right)_{\eta_e}^{n_{e+1}}, \quad r_i^3 = - \left(\psi_i \frac{d\theta}{d\eta} \right)_{\eta_e}^{n_{e+1}},
\end{aligned}$$

where

$$\bar{f} = \sum_{i=1}^2 \bar{f}_i \psi_i, \quad \bar{g} = \sum_{i=1}^2 \bar{g}_i \psi_i.$$

The system of equations after assembly of the elements is nonlinear, therefore an iterative scheme is used to solve it. The system is linearized by incorporating the functions \bar{f} and \bar{g} , which are assumed to be known. Since the whole domain is divided into a set of 40 intervals of equal length, say 0.05, thus we obtain a set of 123 equations with 6 boundary conditions. After applying the given boundary conditions, only a system of 117 equations remains for the solution, which is performed iteratively maintaining an accuracy of 0.0005.

4. Results and discussion

The velocity, microrotation and temperature functions have been computed by using the finite element method and the results are shown graphically in Figs. 1–12. The values of material parameters S , L and A are taken to be fixed at 1.0 each, while m is kept to be fixed at 2.0, and the effect of other important parameters, namely pressure gradient parameter ΔP , micropolar parameter R and surface condition parameter g_o upon these functions has been studied.

Figures 1, 5 and 9 depict the variation of velocity, microrotation and temperature functions with pressure gradient parameter ΔP , while other parameters x , R and g_o are assumed to be fixed as 1.0, 1.0 and 3.0 respectively. Figures 2, 6 and 10 illustrate the variation of these functions with x , while other parameters ΔP , R and g_o are taken to be fixed as 1.0, 1.0 and 3.0, respectively. Figures 3, 7 and 11 show the variation of these functions with micropolar parameter R while other parameters ΔP , x and g_o are fixed as 1.0, 1.0 and 3.0 respectively. Figures 4, 8 and 12 represent the variation of these functions with the surface condition parameter g_o while the other parameters ΔP , x and R are assumed to be fixed as 1.0 each.

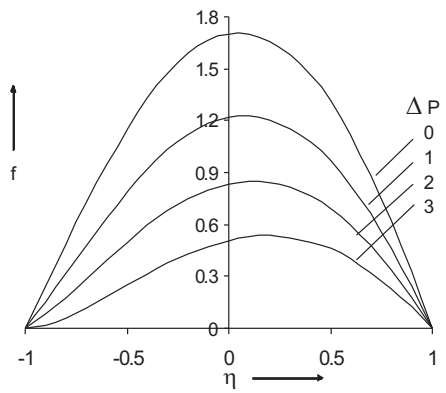


Fig. 1. Velocity distribution for different $\Delta P(x = 1, R = 1, g_o = 3)$.

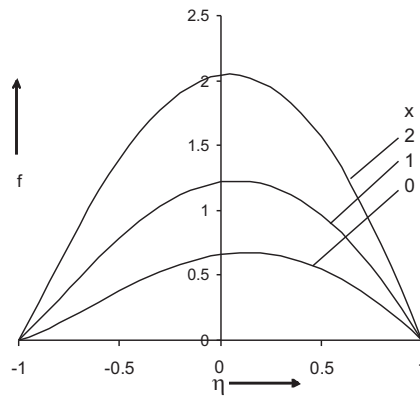


Fig. 2. Velocity distribution for different $x(\Delta P = 1, R = 1, g_o = 3)$.

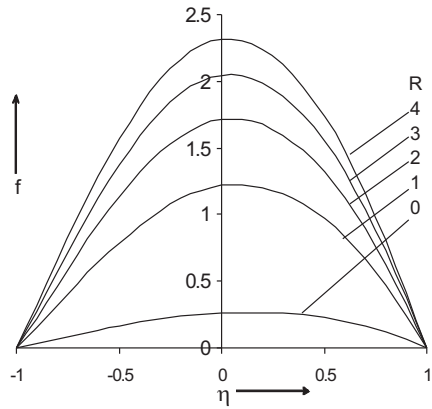


Fig. 3. Velocity distribution for different $R(\Delta P = 1, x = 1, g_o = 3)$.

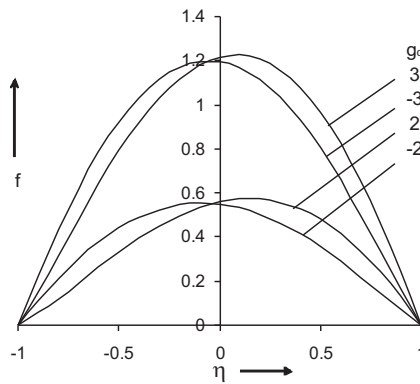


Fig. 4. Velocity distribution for different $g_o(\Delta P = 1, R = 1, x = 1)$.

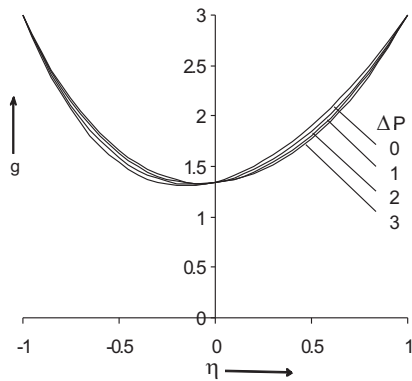


Fig. 5. Microrotation distribution for different $\Delta P(x = 1, R = 1, g_o = 3)$.

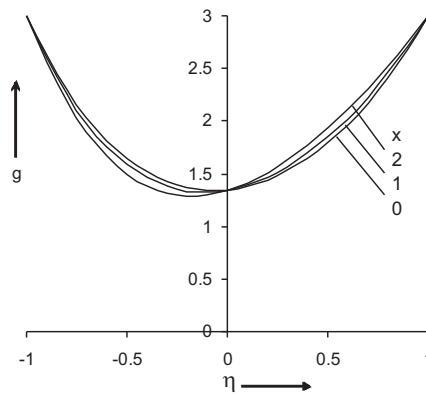


Fig. 6. Microrotation distribution for different $x(\Delta P = 1, R = 1, g_o = 3)$.

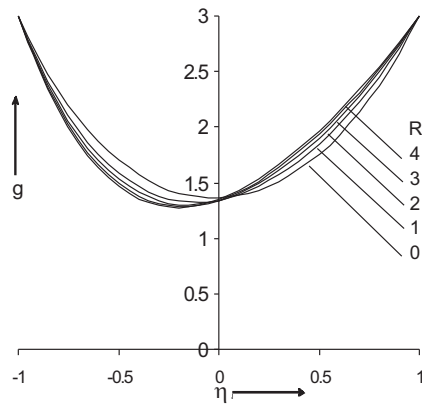


Fig. 7. Microrotation distribution for different $R(\Delta P = 1, x = 1, g_o = 3)$.

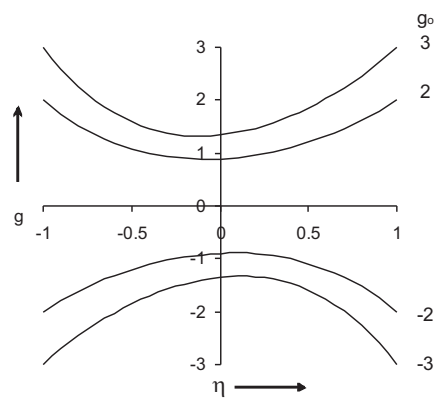


Fig. 8. Microrotation distribution for different $g_o(\Delta P = 1, R = 1, x = 1)$.

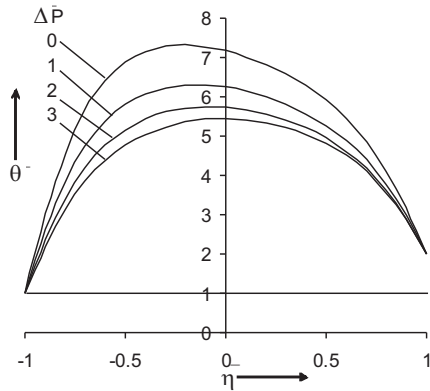


Fig. 9. Temperature distribution for different $\Delta P(x = 1, R = 1, g_o = 3)$.

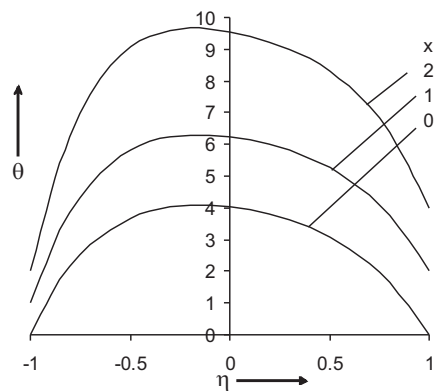


Fig. 10. Temperature distribution for different $x(\Delta P = 1, R = 1, g_o = 3)$.

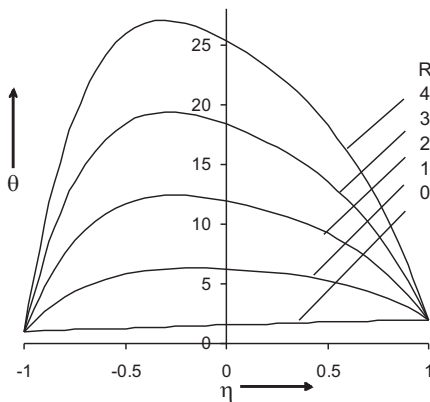


Fig. 11. Temperature distribution for different $R(\Delta P = 1, x = 1, g_o = 3)$.

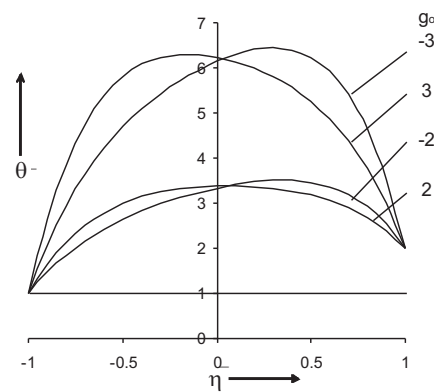


Fig. 12. Temperature distribution for different $g_o(\Delta P = 1, R = 1, x = 1)$.

Figure 1 represents the variation of velocity with the pressure gradient parameter ΔP . The velocity decreases with increases in the pressure gradient parameter ΔP . It is also clear from the figure that with an increase of ΔP , the maxima are shifted towards the right-hand plate ($\eta = 1$). From Figs. 2, 3 and 4, it is observed that the velocity increases with an increase in x , micropolar parameter R and with the absolute value of surface condition parameter g_o . However, the velocity for the Newtonian case ($R = 0$) is sufficiently small as compared to the micropolar fluids ($R \neq 0$). Obviously an increase in g_o shifts the maxima towards the right-hand plate while with increase in the negative value of g_o , the maxima are shifted towards the left-hand plate; which depicts the behaviour of maximum velocity with variable g_o .

Figures 5, 6, 7 and 8 depict the variation of microrotation. Figure 5 shows that in the first half-region, microrotation increases with an increase of the pressure gradient parameter, while it decreases in the second half-region, which is opposite to x and micropolar parameter R as shown in Figs. 6 and 7. From Fig. 8 it is clear that microrotation increases with the increase of the surface condition parameter g_o . It is also clear from the Fig. 8 that for the positive value of g_o , microrotation decreases continuously, until it reaches the minima and then increases continuously, while with the negative value of g_o microrotation increases continuously, until it reaches the maxima and then decreases continuously. Thus the pattern is different for negative and positive values of g_o .

The distribution for the temperature function has been shown in the Figs. 9, 10, 11 and 12. Temperature decreases with the increase of the pressure gradient parameter, while it increases with increasing x the micropolar parameter and with the absolute value of surface condition parameter. Temperature is much lower for Newtonian fluids ($R = 0$) as compared to the micropolar fluids. The temperature distribution is nearly linear for viscous fluids. It is clear from the figures that maximum temperature remains in the first half-region while from Fig. 12 it is observed that for large negative value of g_o , maximum temperature can be obtained in the second half-region.

The variation of skin friction and the rate of heat transfer on both plates with respect to the pressure gradient parameter, micropolar parameter, surface condition parameter and with x are given in Table 1 and 2, respectively.

It is clear from Table 1 that the skin friction numerically decreases with an increase of the pressure gradient parameter ΔP , while it numerically increases with an increase in x , the micropolar parameter R and with the absolute value of surface condition parameter g_o . Thus the skin friction can be effectively reduced by introducing the pressure gradient.

From Table 2 it is observed that the rate of heat transfer numerically decreases with an increasing ΔP , while it increases numerically with the increase of x , the micropolar parameter R and with the absolute value of the surface con-

Table 1. Table for the skin friction $\{f'\}_{\eta=-1,1}$ with different values of the pressure gradient parameter ΔP , micropolar parameter R , surface condition parameter g_o and with x .

| $S = L = A = 1.0, \quad m = 2.0$ | | $\{f'\}_{\eta=-1,1}$ | | | | |
|-----------------------------------|------------|----------------------|---------|---------|---------|---------|
| $R = x = 1, \quad g_o = 3$ | ΔP | 0 | 1 | 2 | 3 | |
| | η | | | | | |
| | -1 | 2.4154 | 1.5319 | 0.8200 | 0.2032 | |
| | 1 | -3.2501 | -2.4446 | -1.7931 | -1.2270 | |
| $\Delta P = R = 1, \quad g_o = 3$ | x | 0 | 1 | 2 | | |
| | η | | | | | |
| | -1 | 0.5626 | 1.5319 | 2.9454 | | |
| | 1 | -1.4165 | -2.4446 | -3.8744 | | |
| $\Delta P = x = 1, \quad g_o = 3$ | R | 0 | 1 | 2 | 3 | 4 |
| | η | | | | | |
| | -1 | 0.3514 | 1.5319 | 2.2379 | 2.7486 | 3.1718 |
| | 1 | -0.6375 | -2.4446 | -3.2543 | -3.7725 | -4.1720 |
| $\Delta P = x = R = 1$ | g_o | -3 | -2 | 2 | 3 | |
| | η | | | | | |
| | -1 | 2.2681 | 1.1315 | 0.5656 | 1.5319 | |
| | 1 | -1.6482 | -0.6964 | -1.2930 | -2.4446 | |

Table 2. Table for the Nusselt number $\{-\theta'\}_{\eta=-1,1}$ with different values of the pressure gradient parameter ΔP , micropolar parameter R , surface condition parameter g_o and variable x .

| $S = L = A = 1.0, \quad m = 2.0$ | | $\{-\theta'\}_{\eta=-1,1}$ | | | | |
|-----------------------------------|------------|----------------------------|----------|----------|----------|----------|
| $R = x = 1, \quad g_o = 3$ | ΔP | 0 | 1 | 2 | 3 | |
| | η | | | | | |
| | -1 | -20.4989 | -16.2988 | -13.7162 | -12.0356 | |
| | 1 | 11.7847 | 9.8791 | 9.0607 | 8.8509 | |
| $\Delta P = R = 1, \quad g_o = 3$ | x | 0 | 1 | 2 | | |
| | η | | | | | |
| | -1 | -12.2673 | -16.2988 | -24.4416 | | |
| | 1 | 9.3425 | 9.8791 | 13.3187 | | |
| $\Delta P = x = 1, \quad g_o = 3$ | R | 0 | 1 | 2 | 3 | 4 |
| | η | | | | | |
| | -1 | -0.5672 | -16.2988 | -37.4175 | -62.0292 | -89.7758 |
| | 1 | -0.4011 | 9.8791 | 20.7529 | 32.5027 | 45.2981 |
| $\Delta P = x = R = 1$ | g_o | -3 | -2 | 2 | 3 | |
| | η | | | | | |
| | -1 | -10.6699 | -4.6916 | -6.3802 | -16.2988 | |
| | 1 | 15.2722 | 5.3884 | 3.7797 | 9.8791 | |

dition parameter g_o . Thus these parameters can be used for controlling the rate of heat transfer. If the plate temperature is higher than the fluid temperature, then the increase in the rate of heat transfer shows that more and more heat is

transferred from the plate to the fluid. This physically means that the cooling effect on the plates increases. Thus fast cooling can be achieved by increasing the micropolar parameter, surface condition parameter and with an increase in x . That is required in polymer industry where after generation of very high temperature, fast cooling is required to achieve a regular structure.

5. Conclusions

1. Velocity decreases with an increase of the pressure gradient parameter, while it increases with an increase in x , with the micropolar parameter and with the absolute value of surface condition parameter. Thus the flow of the fluid can be controlled by simulating these parameters.
2. Pressure gradient parameter ΔP can be used effectively for controlling/simulating the rise in the temperature field.
3. Skin friction numerically increases with increasing values of x , R and g_o while it decreases with ΔP . Thus the drag forces can be reduced by using the pressure gradient parameter.
4. The rate of heat transfer numerically decreases with increasing ΔP , while it increases with an increase in x , micropolar parameter R and with the absolute value of surface condition parameter g_o . Thus fast cooling of the plate can be achieved by increasing the micropolar parameter, the surface condition parameter and with an increase in x . Thus this problem may be very useful in various engineering applications.

Acknowledgment

One of the authors, Lokendra Kumar, is grateful to CSIR, New Delhi for providing a Senior Research Fellowship.

References

1. A.C. ERINGEN, *Simple microfluids*, Int. J. Engng. Sci., **2**, 205–217, 1964.
2. A.C. ERINGEN, *Theory of micropolar fluids*, J. Math. Mech., **16**, 1–18, 1966.
3. T. ARIMAN, M.A. TURK and N.D. SYLVESTER, *Review article-Applications of micro-continuum fluid mechanics*, Int. J. Engng. Sci., **12**, 273–293, 1974.
4. J.W. HOYT and A.G. FABULA, *The effect of additives on fluid friction*, U.S. Naval Ordnance Test Station Report, 1964.
5. V.U.K. SASTRY and V.R.M. RAO, *Numerical solution of micropolar fluid flow in a channel with porous walls*, Int. J. Engng. Sci., **20**, 631–642, 1982.
6. R. BHARGAVA and M. RANI, *Numerical solution of heat transfer in micropolar fluid flow in a channel with porous walls*, Int. J. Engng. Sci., **23**, 409–413, 1985.

7. R.S. AGARWAL, and C. DHANAPAL, *Numerical solution of free convection micropolar fluid flow between two parallel porous vertical plates*, Int. J. Engng. Sci., **26**, 1247–1255, 1988.
8. A.J. CHAMKHA, T. GROŞAN and I. POP *Fully developed free convection of a micropolar fluid in a vertical channel*, Int. Comm. Heat and Mass Transfer, **29**, 1119–1127, 2002.
9. D. SRINIVASACHARYA, J.V.R. MURTHY and D. VENUGOPALAM, *Unsteady stokes flow of micropolar fluid between two parallel porous plates*, Int. J. Engng Sci., **39**, 1557–1563, 2001.
10. R.S.R. GORLA, B. GHORASHI and P. WANGSKARN, *Mixed convection in vertical internal flow of a micropolar fluid*, Int. J. Engng Sci., **27**, 1553–1561, 1989.
11. K.M. NIGAM, K. MANOHAR and S. JAGGI, *Micropolar fluid film lubrication between two parallel plates with reference to human joints*, Int. J. Mech. Sci., **24**, 661–671, 1982.
12. G. ŁUKASZEWICZ, *Micro polar fluids-Theory and Applications*, Birkhauser Boston, 1999.
13. G. AHMADI, *Self-similar solution of incompressible micropolar boundary layer flow over a semi-infinite plate*, Int. J. Engng Sci., **14**, 639–646, 1976.
14. J.S. DAHLER and L.E. SCRIVEN, *Theory of structured continua*, Proc. Roy. Soc., A-275, 504, London 1963.
15. A.D. KIRWAN JR., *Boundary conditions for micropolar fluids*, Lett. Appl. Engng. Sci., **24**, 1237–1242, 1986.
16. J. PEDDIESON JR., *An application of the micropolar fluid model to the calculation of a turbulent shear flow*, Int. J. Engng. Sci., **10**, 23–32, 1972.
17. J.N. REDDY, *An introduction to the finite element method*, McGraw-Hill International Editions, 1984.

Received June 21, 2004; revised version October 29, 2004.
